NAVAL POSTGRADUATE SCHOOL

MONTEREY, CALIFORNIA

THESIS

EXPERIMENTAL STUDY OF COMPOSITES AND METAL-WIRE JOINTS

by

William A. Schultz

September 2008

Thesis Advisor:	Young W. Kwon
Second Reader:	Douglas C. Loup

Approved for public release; distribution is unlimited

THIS PAGE INTENTIONALLY LEFT BLANK

REPORT DOCUMENTATION PAGE			*Form Approved OMB No. 0704-0188*
Public reporting burden for this collection of information is estimated to average 1 hour per response, including the time for reviewing instruction, searching existing data sources, gathering and maintaining the data needed, and completing and reviewing the collection of information. Send comments regarding this burden estimate or any other aspect of this collection of information, including suggestions for reducing this burden, to Washington headquarters Services, Directorate for Information Operations and Reports, 1215 Jefferson Davis Highway, Suite 1204, Arlington, VA 22202-4302, and to the Office of Management and Budget, Paperwork Reduction Project (0704-0188) Washington DC 20503.			
1. AGENCY USE ONLY *(Leave blank)*	**2. REPORT DATE** September 2008	**3. REPORT TYPE AND DATES COVERED** Master's Thesis	
4. TITLE AND SUBTITLE Experimental Study of Composites and Metal-Wire Joints			**5. FUNDING NUMBERS**
6. AUTHOR(S)			
7. PERFORMING ORGANIZATION NAME(S) AND ADDRESS(ES) Naval Postgraduate School Monterey, CA 93943-5000			**8. PERFORMING ORGANIZATION REPORT NUMBER**
9. SPONSORING /MONITORING AGENCY NAME(S) AND ADDRESS(ES) N/A			**10. SPONSORING/MONITORING AGENCY REPORT NUMBER**
11. SUPPLEMENTARY NOTES The views expressed in this thesis are those of the author and do not reflect the official policy or position of the Department of Defense or the U.S. Government.			
12a. DISTRIBUTION / AVAILABILITY STATEMENT Approved for public release; distribution is unlimited			**12b. DISTRIBUTION CODE**

13. ABSTRACT

In order to join a composite structure to a metallic structure, the metal-wire layers were co-cured with composite layers using the Vacuum Assisted Resin Transfer Molding (VARTM). Then, the interface fracture strength was measured for Mode II fracture for various lay-up and interface conditions. The study includes a metal-wire to composite interface, composite to composite interface, and metal-wire to metal-wire interface. In addition, the lay-up orientations of the metal-wires were varied between 0 and 90 degrees. The study also examined the crack propagation from a composite to a metal/composite interface. During the test, the Digital Image Correlation (DIC) technique was applied to capture the strain field around the crack tip. The results suggested that a metal-wire/composite laminate would be effective to connect a composite structure to a metallic structure.

14. SUBJECT TERMS Vacuum Assisted Resin Transfer, VARTIM, Digital Image Correlation, Composite, Fiberglass, Metal Wire, Metal Composite			**15. NUMBER OF PAGES** 51
			16. PRICE CODE
17. SECURITY CLASSIFICATION OF REPORT Unclassified	**18. SECURITY CLASSIFICATION OF THIS PAGE** Unclassified	**19. SECURITY CLASSIFICATION OF ABSTRACT** Unclassified	**20. LIMITATION OF ABSTRACT** UU

NSN 7540-01-280-5500

Standard Form 298 (Rev. 2-89)
Prescribed by ANSI Std. 239-18

THIS PAGE INTENTIONALLY LEFT BLANK

EXPERIMENTAL STUDY OF COMPOSITES AND METAL-WIRE JOINTS

William A. Schultz
Lieutenant Commander, United States Navy
B.S., University of Kansas, 1996

Submitted in partial fulfillment of the
requirements for the degree of

MASTER OF SCIENCE IN MECHANICAL ENGINEERING

from the

NAVAL POSTGRADUATE SCHOOL
September 2008

Author: William A. Schultz

Approved by: Young W. Kwon
Thesis Advisor

Douglas C. Loup
Second Reader

Knox T. Millsaps
Chairman, Department of Mechanical Engineering

THIS PAGE INTENTIONALLY LEFT BLANK

ACKNOWLEDGEMENTS

I would like to thank Professor Young Kwon for all of the support, guidance and patience during the course of my research and graduate studies.

Thanks to the staff at Naval Surface Warfare Center Carderock, including but not limited to Erik Rasmussen, Scot Bartlett, Doug Loup, Tim Dapp, and Paul Coffin, for their continuous support and advice on fabrication and testing for my research.

Finally, I would like to thank my wife Katherine and daughter Caroline for their understanding and support throughout my studies.

THIS PAGE INTENTIONALLY LEFT BLANK

ABSTRACT

In order to join a composite structure to a metallic structure, the metal-wire layers were co-cured with composite layers using the Vacuum Assisted Resin Transfer Molding (VARTM). Then, the interface fracture strength was measured for Mode II fracture for various lay-up and interface conditions. The study includes a metal-wire to composite interface, composite to composite interface, and metal-wire to metal-wire interface. In addition, the lay-up orientations of the metal-wires were varied between 0 and 90 degrees. The study also examined the crack propagation from a composite to a metal/composite interface. During the test, the Digital Image Correlation (DIC) technique was applied to capture the strain field around the crack tip. The results suggested that a metal-wire/composite laminate would be effective to connect a composite structure to a metallic structure.

THIS PAGE INTENTIONALLY LEFT BLANK

TABLE OF CONTENTS

THIS PAGE INTENTIONALLY LEFT BLANK

LIST OF FIGURES

THIS PAGE INTENTIONALLY LEFT BLANK

I. INTRODUCTION

A. BACKGROUND

Current surface ship and submarine construction is progressing toward the use of composite structures to reduce weight and bulk of various structures contained on these vessels. The United States Navy's progression to construct future submarine sails and surface ship superstructures from composites requires more study of the metal composite interface. Existing methods of bonding composites to a metal sub structure use either a mechanical (bolted joint), bonded joint or a hybrid between the two. The best joint efficiency has been a hybrid, mechanical and bonded joint, which is around 60 percent of the base composite material. This is still far below the current technology in metal to metal welded joints.

Bonded and mechanical joints are inherently weak due to internal stress concentrations at the joining surfaces. These stress concentrations are the weakest points and provide the initiation sites for failure. Fabricating a smoother transition, by the use of a co-cured composite/metal wire structure for the joint, will reduce the stress concentrations, increase the load bearing area and increase the joint strength. In order to increase the contact area and avoid using a third material as a bonding agent, the fiberglass woven roving can be interlaced with a metal wire mat which can eventually be joined by welding or casting, providing a significant improvement in the joint efficiency.

Interlacing the fiberglass mat with the metal wire mat creates several different sub joint types within the co cured metal wire and fiberglass joint. Each of these sub joints creates possible failure point. In order to fully understand the co cured metal and fiberglass joint, it must be broken down into each of the respective joints in order to determine which sub joint is the limiting factor. This research investigates some of the possible sub joint types to determine the failure mode, compliance and relative strength, thus giving an idea for future research on overall joint efficiencies.

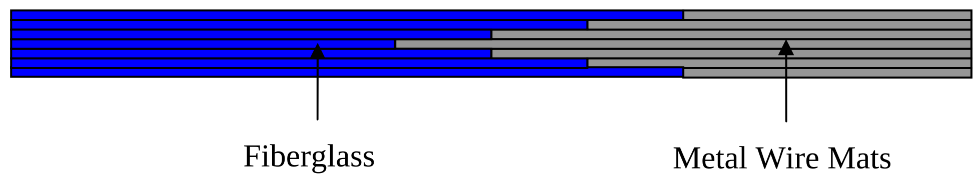

Figure 1. Basic Transition Joint

The basic co-cured metal wire and fiberglass joint consists of layers of E-glass and layers of metal wires which are interlaced and gradually transition from the fiberglass to the metal wire until all of the fiberglass has been transitioned out and there is sufficient metal wire where the joint can be transitioned to a metal structure, Figure 1.

B. OBJECTIVES

The objective of this research is to further initial research completed by Naval Surface Warfare Center Carderock and The United States Naval Academy, [1], in the co-cured metal fiberglass joint. This work will further decompose the basic joint into several possible sub-joints and failure locations to determine the limiting sub-joint type.

The goal is to determine the critical areas of a co-cured transition joint consisting of E-glass to metal wire mat. The experimentation examines different combinations, calculates each of their Mode II inter laminar fracture toughness and compares them to determine the critical combination.

The testing is intended to find possible failure strength and modes by using different orientations and combinations of the fiberglass mat and wire mat layers. Varying the direction of the metal wires, placement of the metal wire backing which was used to hold the wire mat together, location of the crack and number of layers will determine the failure mode and relative failure strength of the various combinations.

II. COMPOSITE FABRICATION

A. MATERIALS

The co-cured composite samples were made from a combination of five materials, a three part resin, E-glass and the metal wire mat.

The resin consists of Derakane 510A vinyl ester resin [2], mixed with Methyl Ethyl Ketone Peroxide 9 percent (MEKP) and Cobalt Napthenate 6 percent solution (CoNAP). MEKP was used as an initiator which causes the chemical curing reaction. The CoNAP was used to promote, speed up, the reaction to give the desired curing time. All components are mixed based on a percent weight for a nominal one hour cure time at 70 deg F per manufactures directions, [2]. In the tests conducted the Deakane 510A was measured by volume and converted to a weight while the MEKP and CoNAP were measured by weight. The amounts of MEKP and CoNAP are used to change the gel time and have no effect on the composite strength.

Other factors that could affect the curing reaction included ambient temperature and the humidity at which chemicals were stored. The ambient temperature was typically between 60 and 80 degrees F which is within the limits of Derakane 510A and did not adversely effect the cure time. The chemicals were stored in air tight containers to prevent moisture penetration, specifically the MEKP and CoNap which are sensitive to humidity.

E glass is a commercial bidirectional fiberglass woven roving, Figure 2. It is categorized by weight in ounces per square yard, 24 oz per square yard woven roving was used for these tests. It is commonly used in many marine, automotive, furniture and aerospace applications.

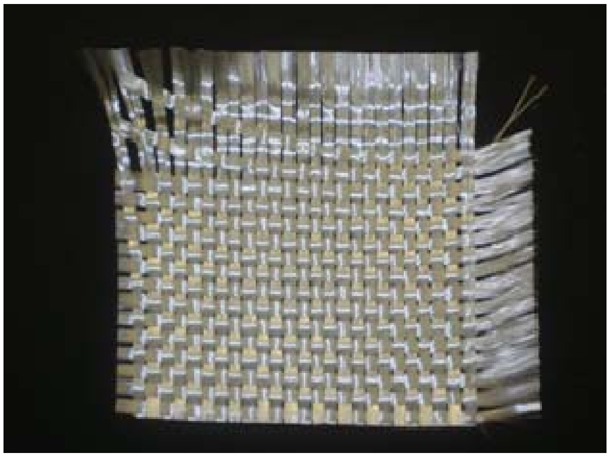

Figure 2. E Glass Woven Roving

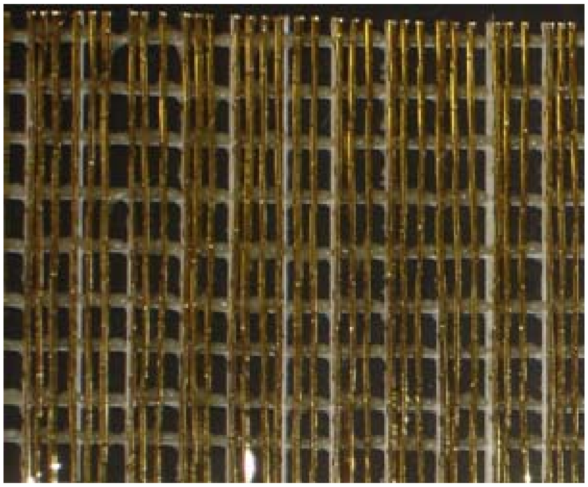

Figure 3. 3SX Metal Wire Mat

The metal wire mat seen in Figure 3 was used in all of the samples. It was a 3SX hardwire with 12 bundles per linear inch fabricated by Hardwire©. The 3SX refers to the three individual wires wrapped by a fourth smaller wire to form a bundle, Figure 3, and they are arranged 12 per inch bound by a fibrous backing.

B. APPARATUS

The composite fabrication apparatus consisted of five major component, the vacuum pump, a resin trap, gauge board, glass sheet which served as the molding surface and the vacuum bag sealing surface and a reservoir to hold the resin, Figure 4.

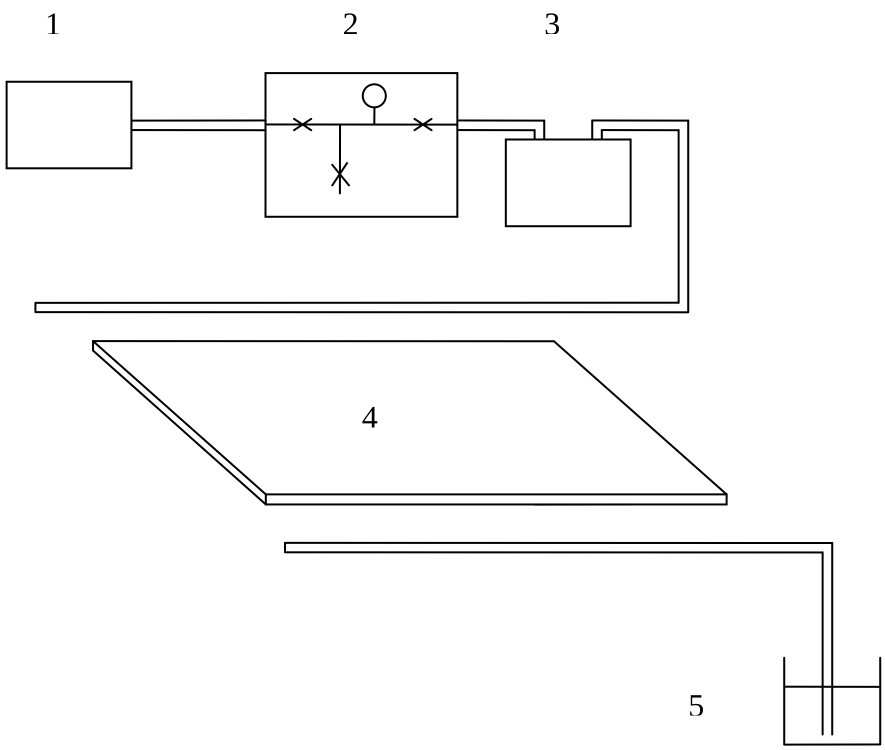

Figure 4. Sketch of Infusion Apparatus

1. Vacuum Pump
2. Gauge Board
3. Resin Trap
4. Glass sheet, vacuum bag assembly and composite
5. Resin reservoir

The vacuum pump is a Rietschel Thomas Vacuum Pump model 2688CE44 capable of maintaining .18 cubic feet per minute flow at 25 inches of mercury vacuum. It provides the initial vacuum to set the composite in place and maintains the vacuum to ambient atmospheric differential pressure to draw the resin through the composite.

Figure 5. Resin Trap

The resin trap, Figure 5, prevents the excess resin from contaminating the gauge board or the vacuum pump. It is made from a glass bowl sealed by a lid with inlet and outlet tubing allowing the resin to fall in to the bowl while allowing the air to pass through to the vacuum pump.

The working surface was fabricated from a sheet of ½ inch thick tempered glass. The glass provides a solid and thermally stable platform for the exothermic reaction to take place. It also allowed for a smooth sealing surface to seal the vacuum bag and provided a rigid molding surface for the composite laminate.

A gauge board, Figure 6, was used to measure, regulate and hold the vacuum. It was made from two ball valves, for isolation, one needle valve, to regulate the vacuum, and a vacuum gauge for observation of the vacuum. The vacuum was connected to the fitting of the right side of the gauge board, measured by the gauge in the center and regulated by the needle valve at the bottom center, Figure 6.

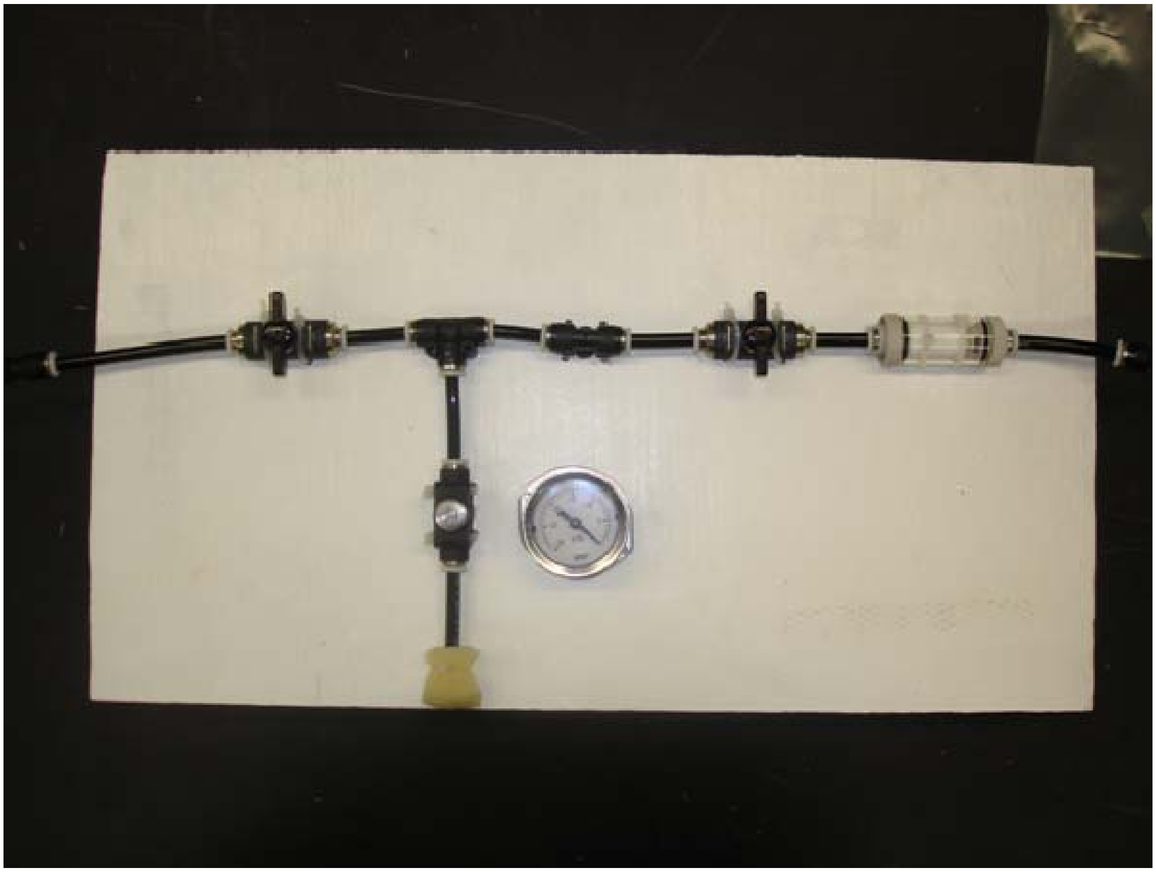

Figure 6. Gauge Board

Resin was mixed and degassed in a plastic bucket and isolated from the system by crimping the polyethylene tubing with a set of sheet metal vice grips while the vacuum was being established and tested. After a satisfactory vacuum was established the sheet metal vice grips were removed allowing the resin to flow on to the composite coupon.

C. GENERAL COMPOSITE COUPON FABRICATION

Each composite coupon was formed by the same general method. The only variation was the individual layers and orientation of the E-glass and metal wire mat layers. The molding surface of the tempered glass sheet was cleaned and inspected for defects that may have produced any surface discontinuities on the composite. A piece of distribution media roughly the same size of the coupon was placed on the molding

surface and covered with a layer of release film. The release film was cut large enough to encapsulate the composite coupon to prevent the coupon from adhering to anything else. Next the desired layers of E-glass and metal wire mat were layered on the release ply in the desired orientations ensuring the composite coupon was completely on the release ply while being offset about 1 inch from the distribution media, as shown in Figure 7. The offset of the distribution medium at the resin inlet allowed the spiral cut tubing to distribute the resin across the entire edge of the coupon while the overlap of the distribution medium with the coupon at the outlet tube prevented the resin from bypassing the coupon through the distribution media and not infusing across the composite coupon. Sections of spirally cut tubing were attached to the inlet and outlet tubes. The spirally cut tube section's length matched the length of the composite coupon side. Each of spirally cut sections were laid out along opposing edges of the composite coupon. Both tubes rested on the lower release ply layer, with the inlet tube having the distribution media directly below the release ply layer and approximately ¼ inch from the composite coupon. The outlet spirally cut tube rested on the release ply immediately adjacent to the edge of the composite coupon. A second piece of release ply, similar in size to the first one, was placed on top the assembled composite coupon. On top of the release ply a second layer of distribution media, with similar dimensions, was placed in the same orientation as the one under the composite coupon, aligned ¼ inch from the spirally cut tube at the inlet and directly adjacent to the composite coupon on the outlet. The entire assembly was taped in place with duct tape and the edges were lined with vacuum bag tape on the glass approximately 6 inches from the edge of the peel ply. Vacuum bag tape was also placed around the inlet and outlet tubes where it crossed the vacuum bag tape on the glass. A vacuum bag was rolled over the entire assembly and sealed by the vacuum tape. Tabs made from the vacuum bag tape, were placed adjacent to the inlet and outlet tubes to allow the vacuum bag to be pleated which allowed the bag to cover and conform to the varying thickness of the composite layup and inlet and outlet tubes without bridging. This completed the vacuum bag assembly, Figure 8.

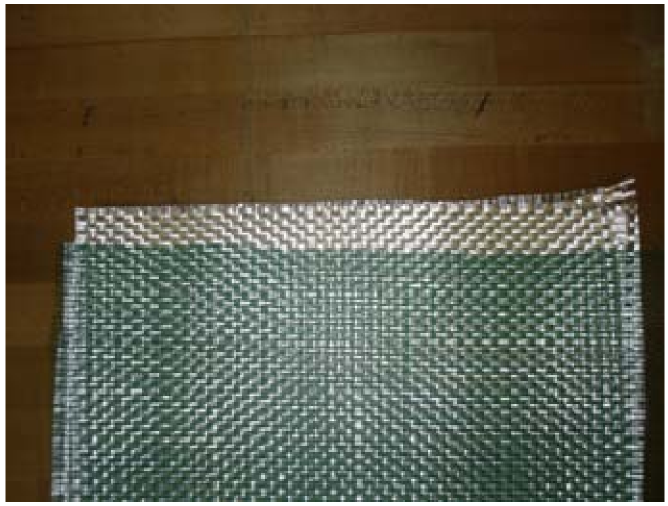

Figure 7. Distribution Media Offset

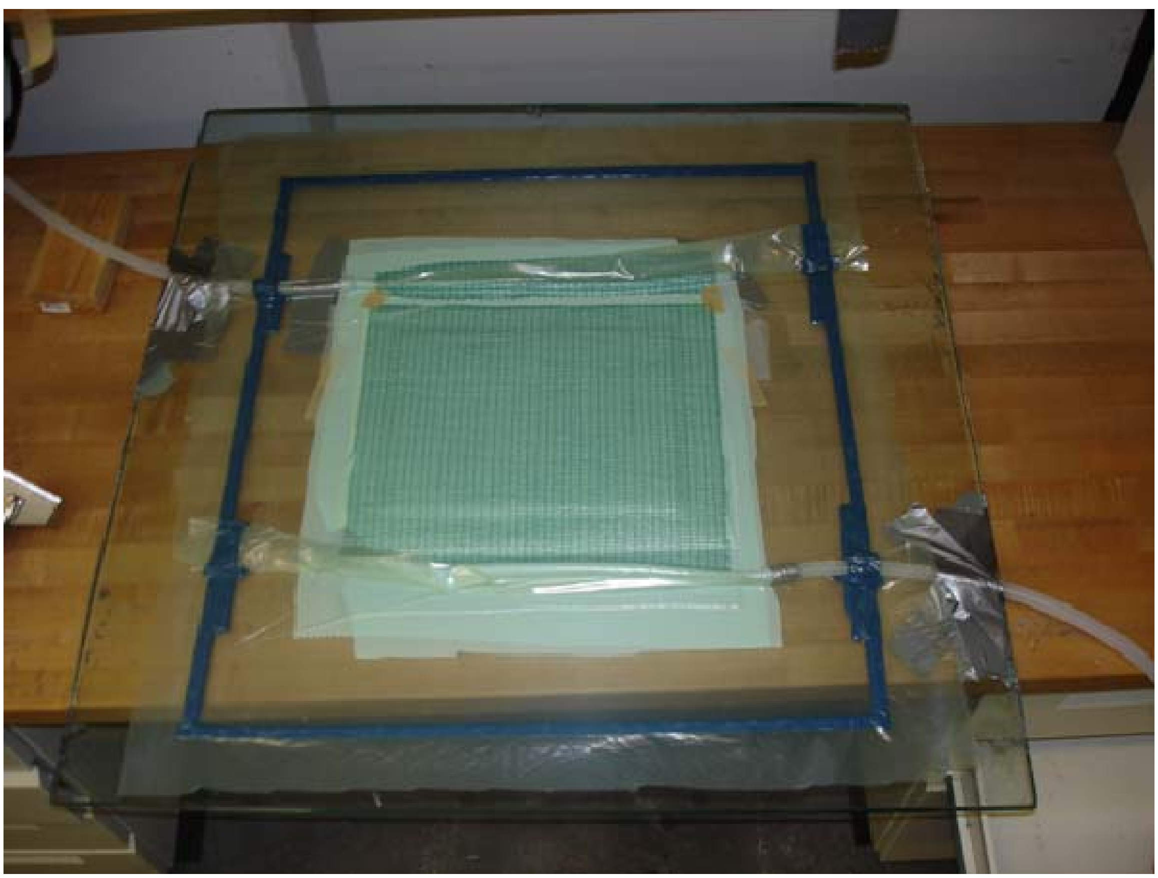

Figure 8. Completed Vacuum Bag Assembly

The vacuum test was started by turning the vacuum pump on and clamping the resin inlet tube with a set of sheet metal vice grips. This allowed the vacuum bag to compress the composite coupon and form the seal between the vacuum bag tape, sheet of glass and the vacuum bag. As the vacuum was drawn creases were worked out of the vacuum bag by moving the creased portion of the bag to non critical locations, off the composite coupon and vacuum leaks were sealed. Once a satisfactory vacuum had been established the valves on the gauge board were used to isolate the vacuum pump from the system and a vacuum test was performed to ensure that the vacuum bag would maintain vacuum pressure indicating there were no vacuum leaks in the bag and tubing system. Upon successful completion of a vacuum test the valve to the vacuum pump was reopened allowing the vacuum pump to maintain the vacuum.

The resin was mixed in accordance with the manufacturer's directions, [2] to achieve the desired gel or cure time. In this case the resin was measured by volume and the CoNAP and MEKP were measured by weight. The MEKP was added to the Derakane 510A and mixed to produce a light brown haze color. Then the CoNAP was added and mixed. One note of caution the MEKP and CoNAP should never be mixed together and explosion or violent reaction may result. After the resin, promoter and initiator were mixed they were allowed to sit for 10 minutes. This allowed the reaction to start and degassed the resin mixture to prevent bubbles from entering into the composite coupon. When the vast majority of bubbles surfaced, about 10 minutes, the resin was ready to be introduced in to the composite coupon. The resin bucket was placed below the sheet of glass containing the composite coupon and the inlet tube was immersed in to the resin bucket.

The sheet metal vice grips were released allowing the resin to be drawn up the inlet tube and across the composite coupon's edge. The resins advance was monitored by viewing the resin front from the top, bottom or back lighting from the bottom. When the composite coupon was fully infused and the resin started to exit into the outlet tube the inlet tube was secured with the sheet metal vice grips, stopping the flow of the resin. The vacuum pump remained on for at least one hour, or longer depending on the resin gel time, to maintain a uniform compaction of the composite coupon until the resin had fully

gelled. When the gel time had elapsed, the outlet tube was clamped with a second set of sheet metal vice grips. The vacuum pump was turned off and the assembly left to continue curing in the sealed vacuum bag for 24 hours. After 24 hours, the composite coupon was removed and cut to the desired specimen sizes. This was performed at an off site location which used a water jet cutter to make the desired sample sizes. Prior to testing, the samples were post cured at 140 deg F for 6 hours to advance resin cure state to a uniform level equivalent to long term ambient temperature cure conditions.

D. SPECIFIC COUPON FABRICATION

The basic co-cured metal wire fiberglass joint was separated into nine individual sub-joint types. Each case was designed and fabricated to represent a possible critical area in the co-cured metal and fiberglass joint. Metal wire orientation, and placement of the crack initiation site were the major variables used to formulate each of the cases. In general these areas represent areas that bond metal to metal with resin, bond fiberglass to metal or major changes in the stiffness of the structure. Critical area one, Figure 9, is located to address the possibility of a crack forming in manufacturing and propagating into the joint and to investigate the possibility of delamination of the fiber glass as a load is applied to the structure. Critical area two, Figure 9, represents the interface boundary between the fiberglass and wire mat. Lastly critical area three, Figure 9, investigates the bond between two layers of wire mat.

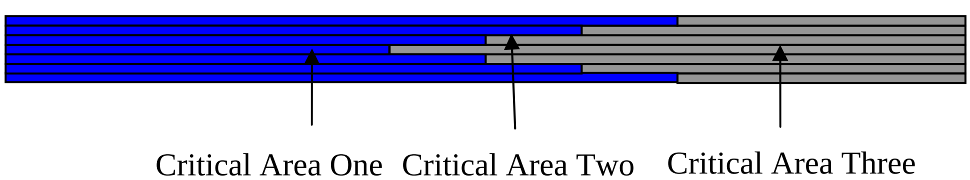

Figure 9. Selected Critical Areas

1. Case 1:

Case 1, Figure 10, consisted of two identical halves of three layers of E-glass woven roving, represented in blue, followed by one layer of hardwire mat, orientated 90 degrees to the crack face or parallel to the longest edge in Figure 10, (called 0 degree layer from now on) with the fibrous backing between the fiberglass and wire mat. Between the two halves and layers of wire was the crack initiation site. In this case a piece of Teflon film was used to separate the two layers of wire and prevent bonding by the infused resin. Figure 10 represents the three layers of fiberglass in blue, the fibrous backing on the hardwire mat in yellow and hardwire mat in brown. Note the crack is initiated at the right side and protrudes into the sample.

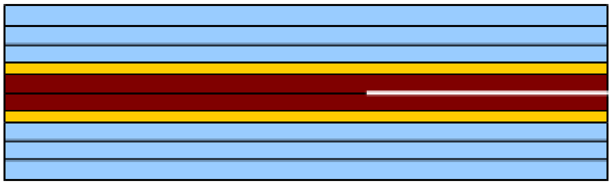

Figure 10. Case 1

2. Case 2

Case two investigated how a crack would propagate into the tip of the co-cured joint. It consists of four layers of fiberglass followed by a layer 0 degree metal wire mat with the fibrous backing side down and four more layers of fiberglass to maintain symmetry. Figure 11 represents Case 2, the blue layers represent 4 layers of fiberglass above and below the crack, metal wire mat is brown and the fibrous backing is yellow. For Case 2 the distance from the crack tip to the wire mat was 1 inch.

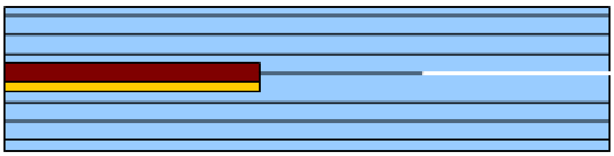

Figure 11. Case 2

3. Case 3

Case three, Figure 12, was identical to Case two, as seen in Figure 11, except the metal wire mat was orientated parallel to the crack face or the wires were running in to and out of the paper (called 90 degree layer from now on).

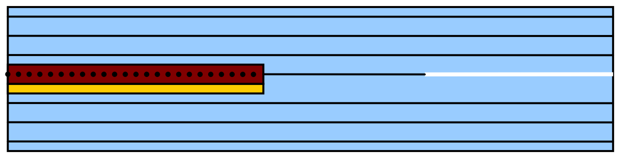

Figure 12. Case 3

4. Case 4

Case four, Figure 13, was identical to Case one, Figure10, except that the metal wire mat was 90 degree layer.

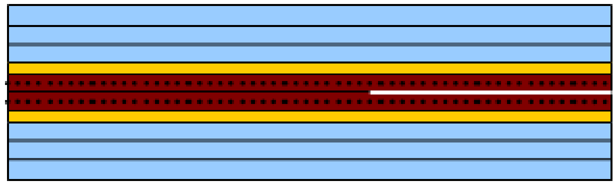

Figure 13. Case 4

5. Case 5

Sample Case five consisted of four layers of fiberglass, a crack initiation site and four more layers of fiber glass represented in Figure 14.

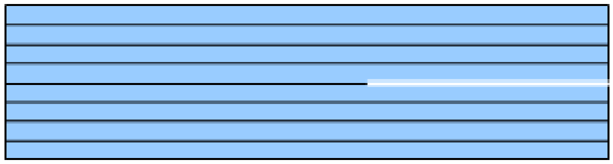

Figure 14. Case 5

6. Case 6

Case six was similar to Case 1 except the metal wire mat was inverted so the fibrous backings were facing each other. Figure 15 shows the fiberglass in blue, wire mat in brown, and the backing layers in yellow.

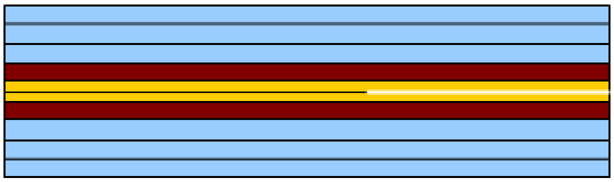

Figure 15. Case 6

7. Case 7

Case seven, Figure 16, was identical to Case two, Figure 11, except the distance between the crack tip and the wire mat was 0.25 inches.

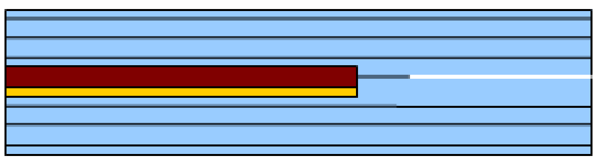

Figure 16. Case 7

8. Case 8

Case eight was similar to Cases one and four, with the two sheets of wire mat aligned at 90 degrees to each other. The layup is represented schematically in Figure 17 with. The top wire mat was set with fibrous backing facing up and the wire bundles at a 90 degree orientation. The second layer of wire mat was set with the fibrous backing side down and the wire mat running parallel with the long edge in a 0 degree orientation.

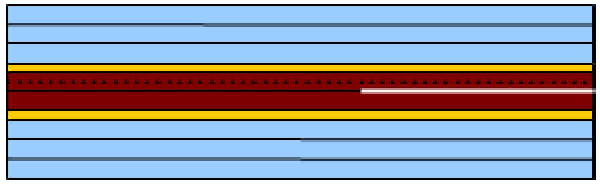

Figure 17. Case 8

9. Case 9

Case nine was the only asymmetric case tested. It had 4 layers of fiberglass followed by the crack initiation site, then a layer of wire mat with the fibrous backing facing up and followed by two more layers of fiberglass, Figure 18. Care was taken to ensure the neutral axis was as close as possible to the geometric center of the thickness. Figure 18 illustrates the layout of this sample.

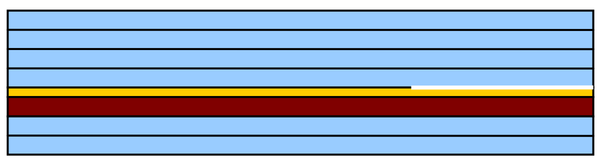

Figure 18. Case 9

10. Case 10

Case 10 was identical to Case three except the crack tip began at the wire's edge, Figure 19.

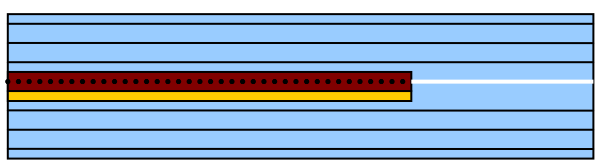

Figure 19. Case 10

11. Case 11

Case eleven was similar to Case four except the two fibrous backings were facing each other in the center of the sample, Figure 20.

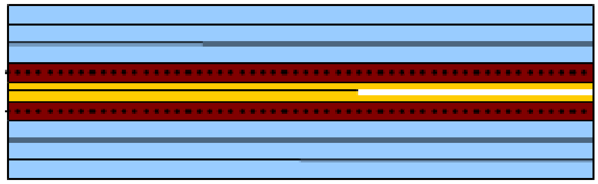

Figure 20. Case 11

12. Case 12

Case twelve was similar to Case one except the fibrous backing for both layers of wire mat were facing up, Figure 21.

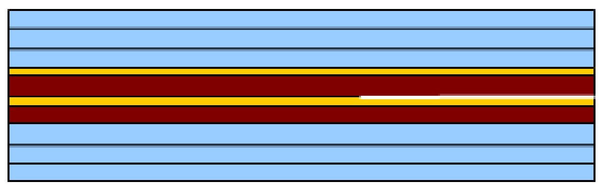

Figure 21. Case 12

III. TESTING

A. APPARATUS

Static fracture Mode II tests were conducted on each of the samples using an Instron 4507 testing system. The samples were placed in a three point bending system, Figure 22, and load and displacement data were recorded. In addition to the load and displacement data, the image correlation software, produced by Correlated Solutions, was used to view the strain fields on the samples' surface.

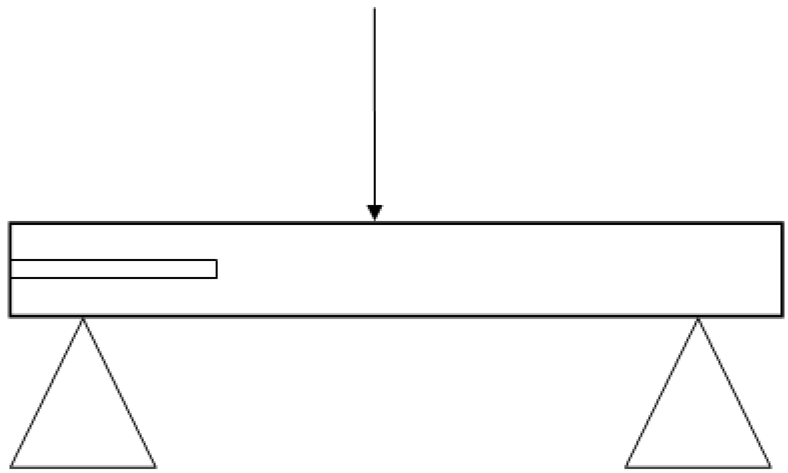

Figure 22. Three Point Bending System

B. PROCEDURE

Each sample was tested for Mode II interlaminar toughness by placing it in a three point bending stand. The distance from the crack tip to the support on the right side was 4.5 cm and the distance between the two supports was 18 cm. The load was applied at the center between the two supports. For these samples Instron 4570 held the center support stationary with the load cell and moved the two lower supports up into the stationary support connected to the load cell. Figure 23 shows a fully dimensioned test setup. Digital image correlation software was simultaneously used and recorded deformation fields on the surface near the crack tip.

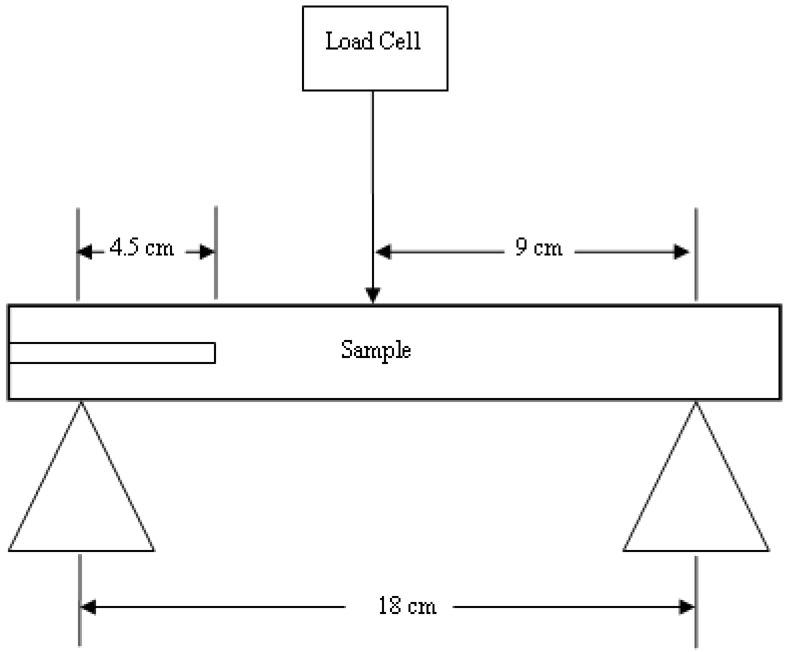

Figure 23. Dimensioned Test Setup

IV. INTER LAMINAR FRACTURE TOUGHNESS CALCULATIONS

Inter laminar fracture toughness calculations, G, were performed on each sample by simplifying the equations provided from, [3]. Equations 1 and 2 were simplified by assuming the compliance or slope of the load versus displacement graph was linear, until crack propagation occurred. Assuming the compliance, the inverse of the slope load vs. displacement graph was constant, C_1=C_0, reduces Equation 2 to a_1= a_0. Combining Equations 1 and the simplified Equation 2 results in the interlaminar fracture toughness, Equation 3, where a is the distance from the crack tip to the support, L is the length of the sample, B is the width of the sample, P was the load applied just prior to the failure and C was the compliance, Figure 24. The compliance was derived from the inverse of the slope of the load vs. displacement graph just prior to failure or crack propagation.

$$G = \frac{9a^2P^2C_1}{2B(2L^3 + 3a_1^3)}$$

Equation 1

$$a_1 = \left[\frac{C_1}{C_0} a_0^3 + \frac{2}{3}\left(\frac{C_1}{C_0} - 1 \right) L^3 \right]^{\frac{1}{3}}$$

Equation 2

$$G = \frac{9a^2P^2C}{2B(2L^3 + 3a^3)}$$

Equation 3

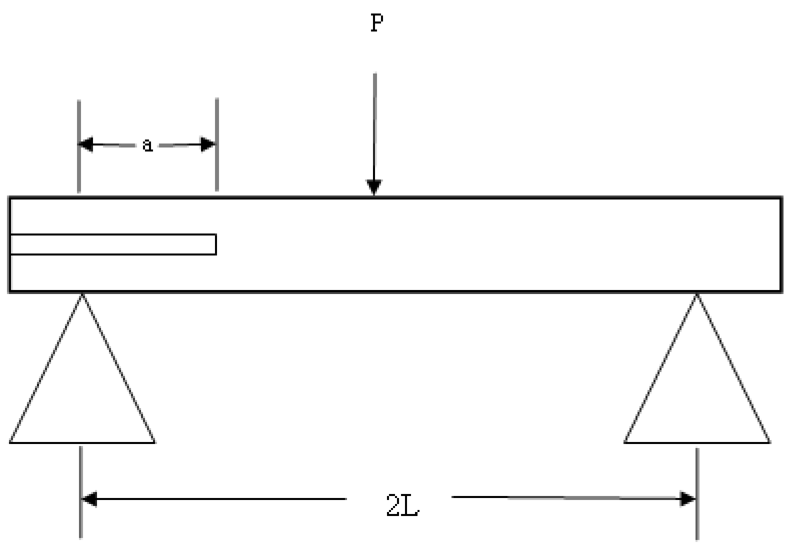

Figure 24. Equation Variables

V. RESULTS

This research investigated several different internal configurations of the co-cured composite/metal hybrid joint. Each sample was evaluated for the failure mode and interlaminar fracture toughness, G. Results from interlaminar fracture toughness calculations are shown in Figure 25, note the error bars show one standard deviation. Averages and standard deviations from each of the case groups were computed. Some samples were excluded due to equipment failure. Another common failure was movement of the support stand. A total of at least seven samples were tested for each case and the fracture toughness values represent an average of at least five samples. Figures 26 and 27 provide a brief summary of all twelve cases.

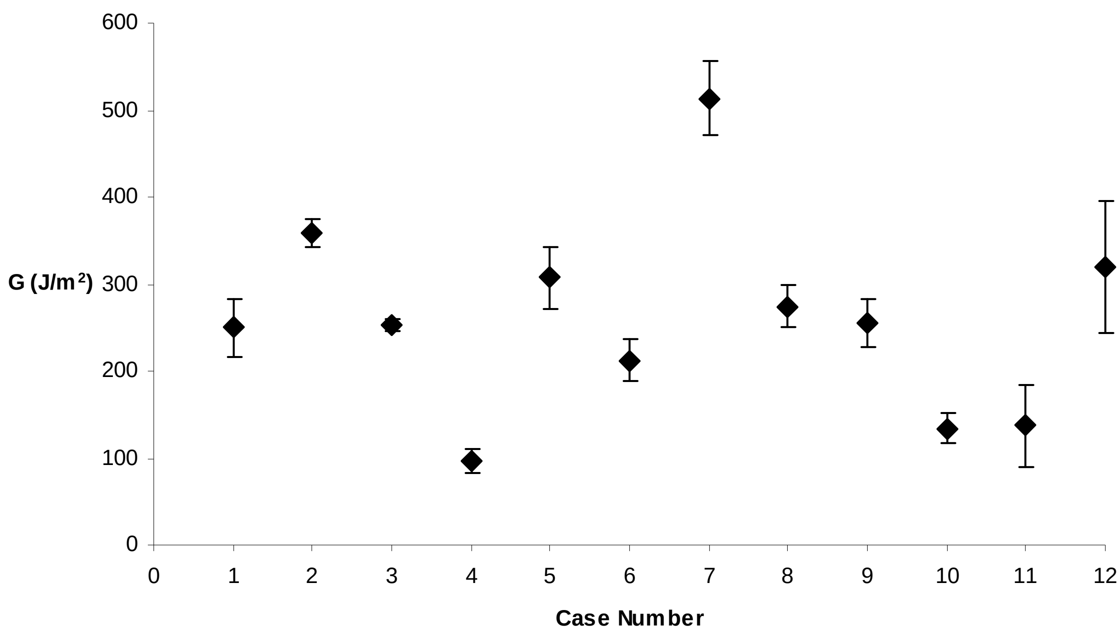

Figure 25. Summary of Energy Release Rate vs. Case Number

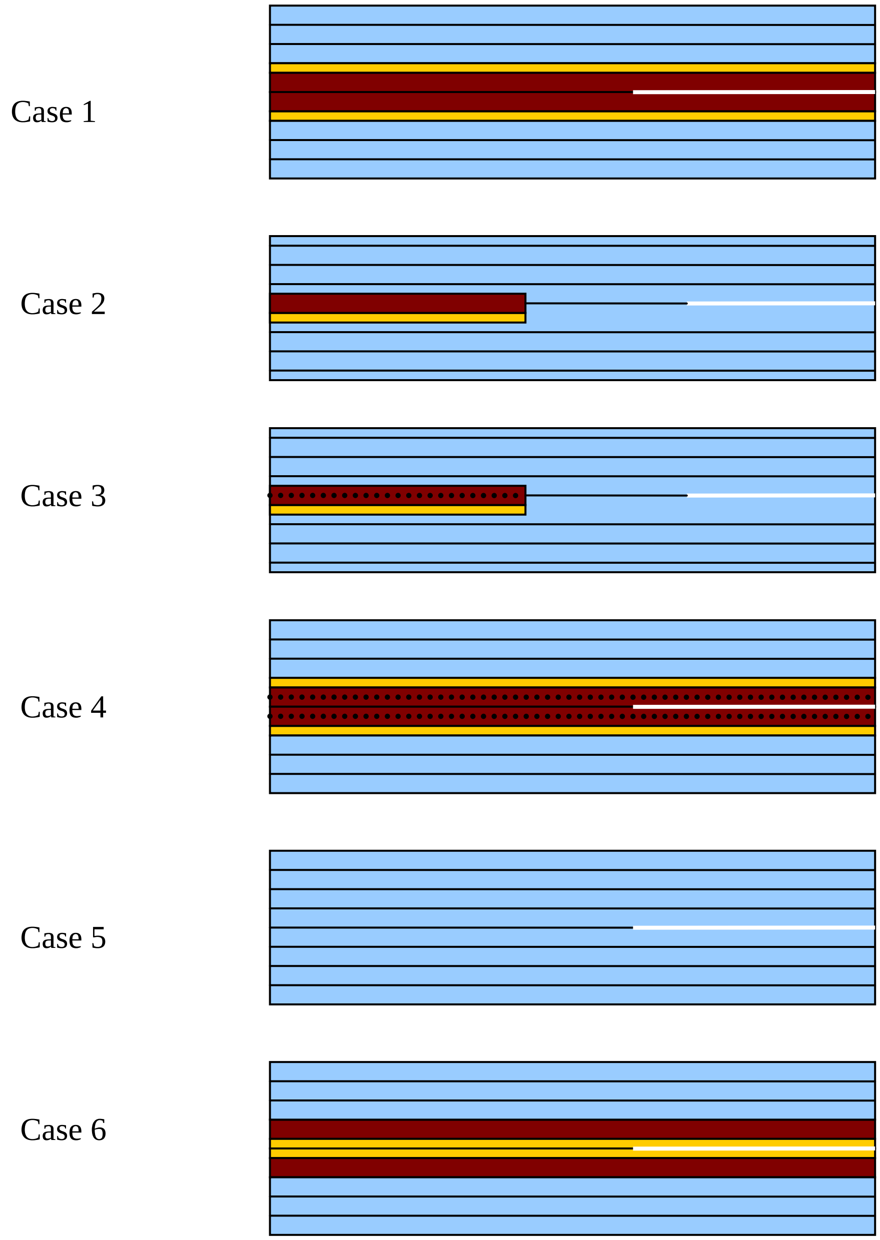

Figure 26. Summary of Cases one through six

(Blue indicates a composite layer, red denotes a metal wire layer, yellow is the plastic backing of the metal wire layer, and dots represent the 90 degree layer of the metal-wire layer.)

Case 7

Case 8

Case 9

Case 10

Case 11

Case 12

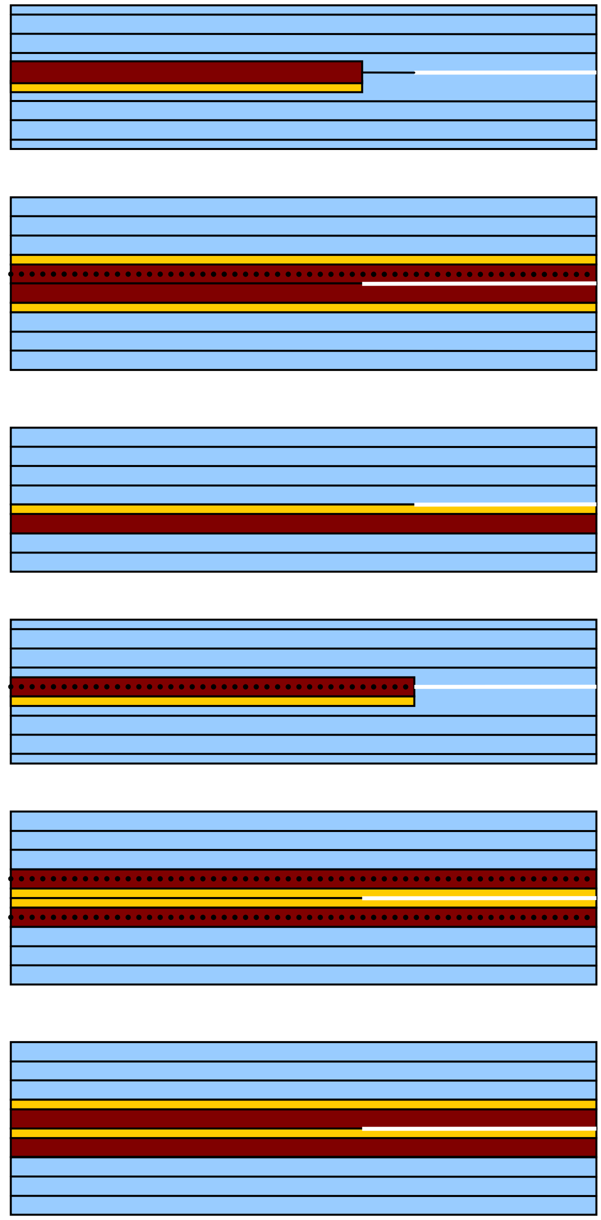

Figure 27. Summary of Cases seven through twelve

(Blue indicates a composite layer, red denotes a metal wire layer, yellow is the plastic backing of the metal wire layer, and dots represent the 90 degree layer of the metal-wire layer.)

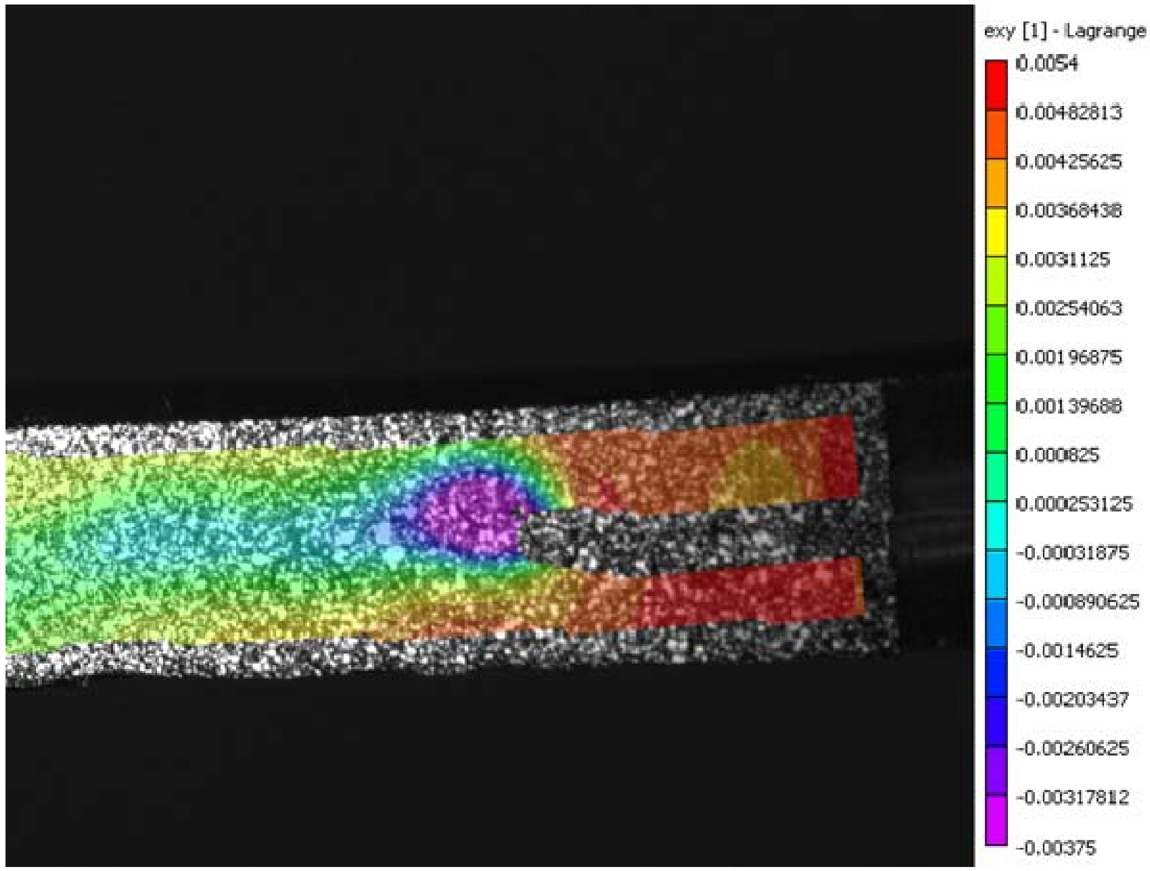

Figure 28. Typical Failure and Crack Initiation

A. FAILURE MODE

First each sample was evaluated for the mode of failure. In all cases the primary failure mode was shear along the neutral axis. Figures 28 and 29 provide representative examples of this failure. To illustrate the buildup of stress, the digital image correlation software has been superimposed to provide the inplane shear strain e_{xy} on top of the picture of the specimen.

Both Figures 28 and 29 illustrate the typical failure in shear. Secondary bending failures occurred on tests that were allowed to continue beyond the initial shear failure, Figure 30. These failures occurred at the maximum deflection of the sample between the crack front and the midpoint of the specimen because the initial failure at the crack face caused a decrease in the cross sectional moment of inertia for the cracked beam section.

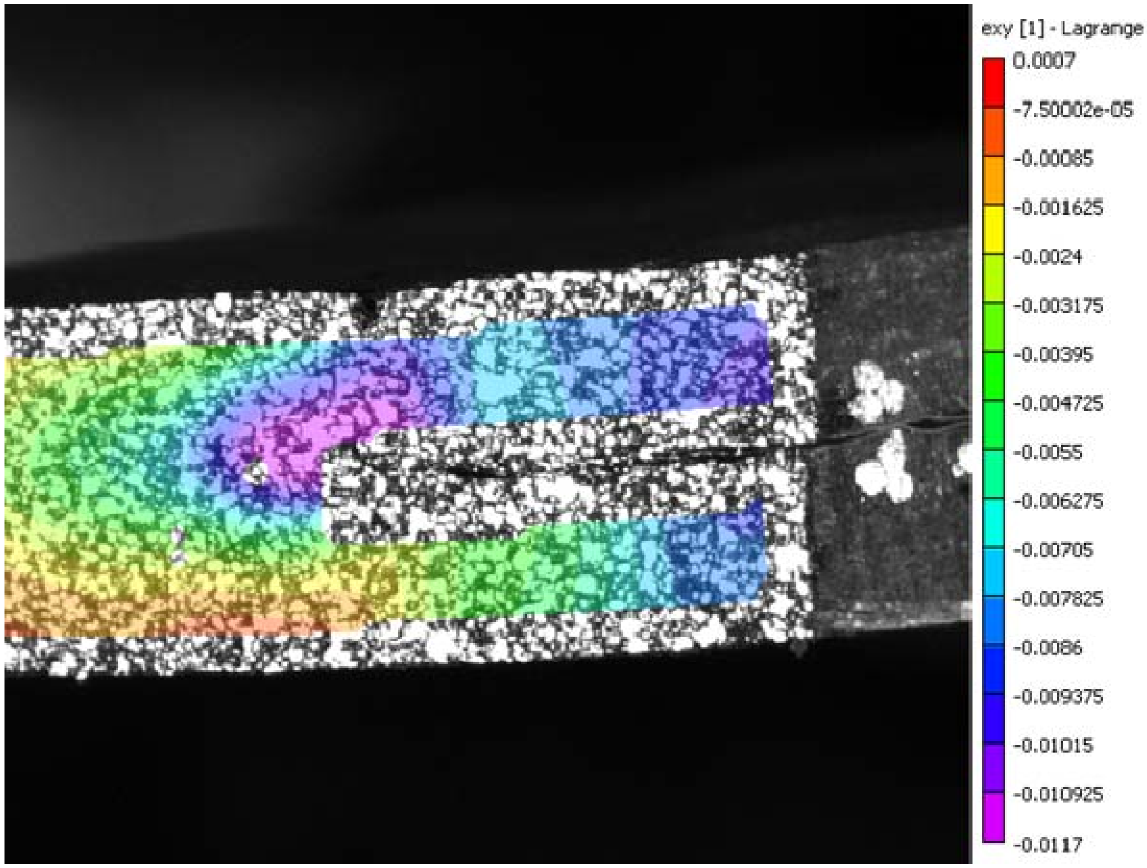

Figure 29. Typical Failure, Crack Initiation and Propagation

Samples with the metal wire mat of the 90 degree layer failed in shear, as expected. Then the crack propagated up between the wire bundles, Figure 31, continuing to propagate between the wire mat and fiberglass layers.

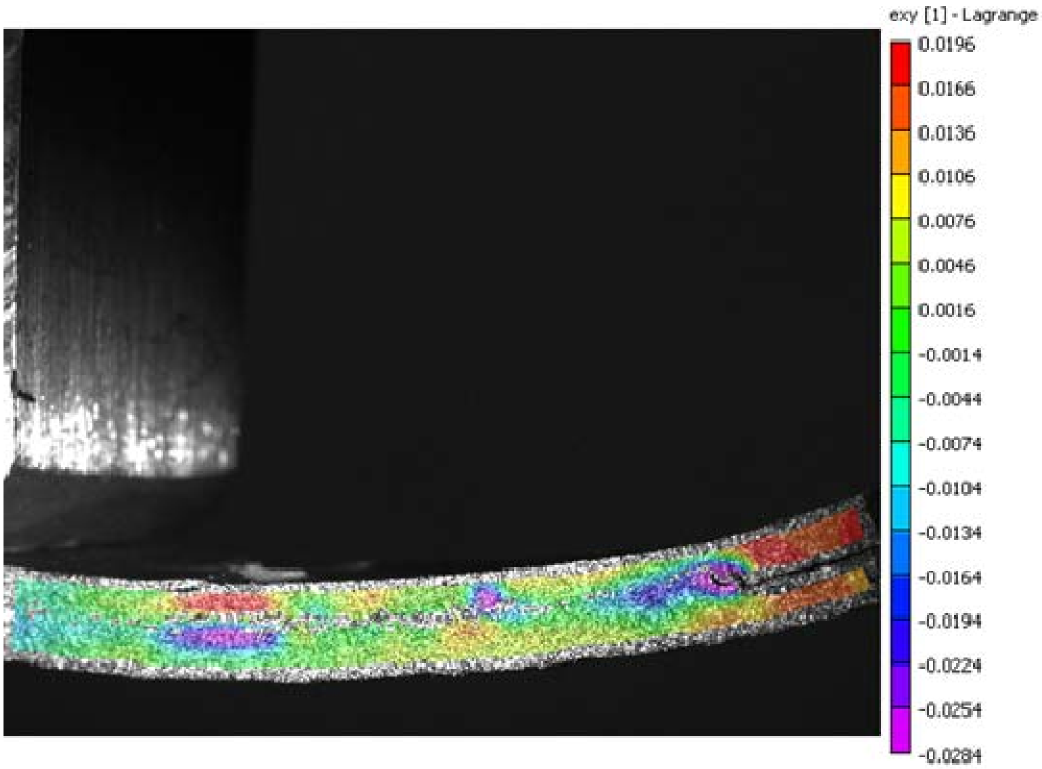

Figure 30. Crack Propagation and Failure by Bending

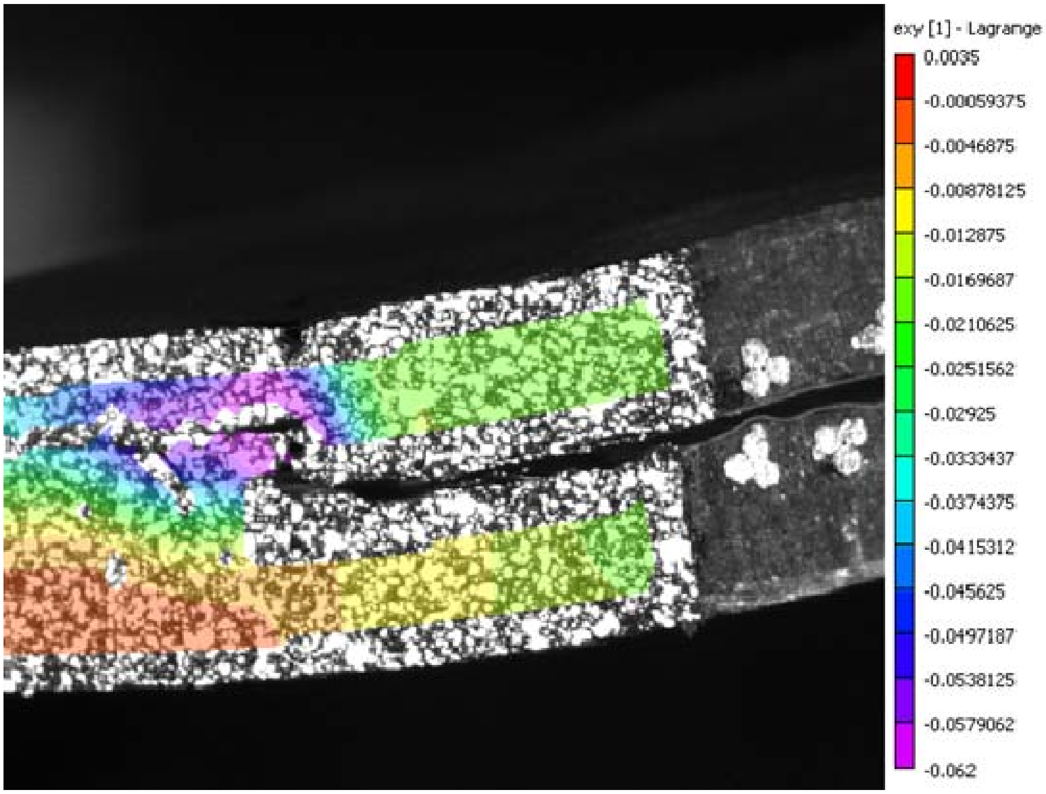

Figure 31. Crack Propagation Through the Wire Layer

B. INTER LAMINAR FRACTURE TOUGHNESS

Interlaminar fracture toughness was calculated for each sample. A summary of the individual cases with error bars equaling one standard deviation is shown in Figure 25. Not all samples were included in the final graph due to errors in the data, usually caused by test stand movement during the performance of the test. As seen in Figure 25, Case 4, which had an interface crack between the two 90 degree metal wire layers, resulted in the lowest fracture toughness among all cases.

Comparison of Case 1 with metal wire mat of 0 degree to Case 4 with metal wire mat of 90 degree layer proved the wire mat of 90 degree layer is the weakest configuration as shown in Figure 32, even though both had wire to wire contact at the crack initiation site. This was further supported by viewing and comparing Cases 2 and 3, both of which had a 1 inch gap between the crack face and the crack initiation point.

While Case 2 had the wire mat of 0 degree layer, Case 3 had the wire mat of 90 degree layer. Among the two, Case 3 had lower fracture toughness.

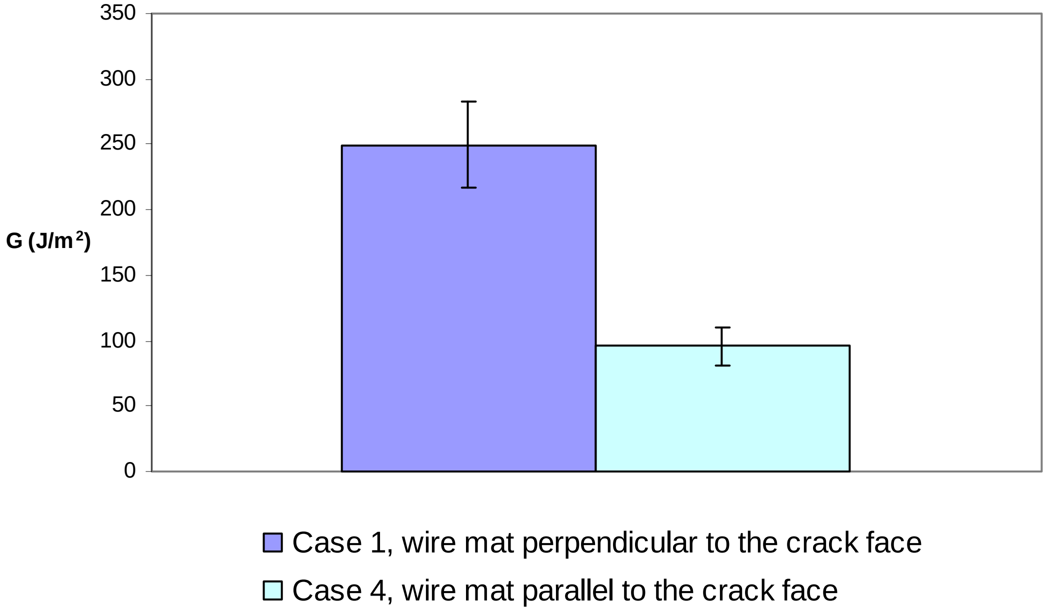

Figure 32. Average Fracture Toughness Cases 1 and 4 with one Standard Deviation

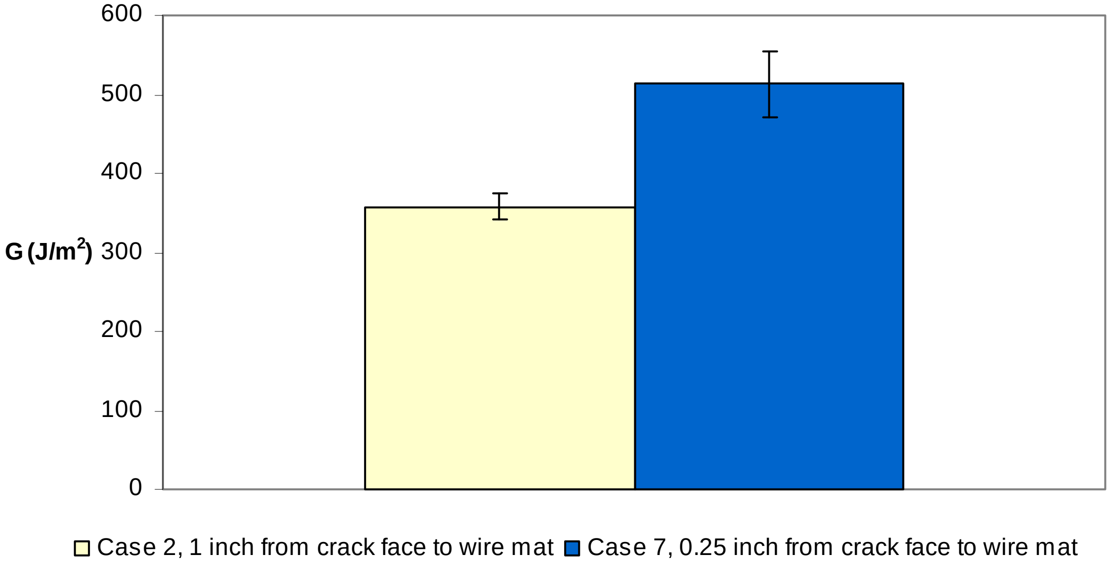

Figure 33. Average Fracture Toughness Cases 2 and 7 with one Standard Deviation

Case 5, which had eight layers of fiber glass with a crack initiation site in the middle, served as a verification of the material properties. Comparing Case 5 to the other cases illustrated in the majority of the cases the addition of the wire mat decreased the interlaminar fracture toughness compared to a uniform fiber glass sample.

Figure 33 compares Cases 2 and 7, both with 0 degree metal wire orientation, which varied by the distance between the crack tip and metal wire mat. Case 7 proved to be stronger due to the increased stiffness of the imbedded wire mat. Furthermore Case 2 with 0 degree layer face wire mat had a higher interlaminar fracture toughness than Case 3 which had the weaker 90 degree wire mat layer configuration with the same distance from the crack to the wire mat, Figure 34. In general the lower interlaminar fracture toughness was produced by the greater distance between the crack face and metal wire mat and the lowest was produced by the greatest distance between the crack face and the wire mat with a 90 degree orientation, Case 3.

Comparing Cases 1 and 6 (0 degree orientation) and 4 and 11 (90 degree orientation), Figure 35, showed the fibrous backing has little effect on the fracture toughness. It also restates the conclusion the 90 degree wire mat orientation had a lower fracture toughness when compared to the 0 degree orientation.

In general comparing Cases 3, 4, 10 and 11 (90 degree wires) to Cases 1, 2, 5, 6, 7 and 12 (either 0 degree wires or no wires) shows 90 degree wire orientation has a lower fracture toughness, Figure 25. The exception to this is Case 3. However, the wires in Case 3 start one inch from the crack tip and in the testing the crack never interacted with the wires until after the initial failure point where the fracture toughness would be calculated. Subtracting Case 3 gives the conclusion 90 degree wire reinforced composites are weaker than 0 degree wire reinforced composite structures.

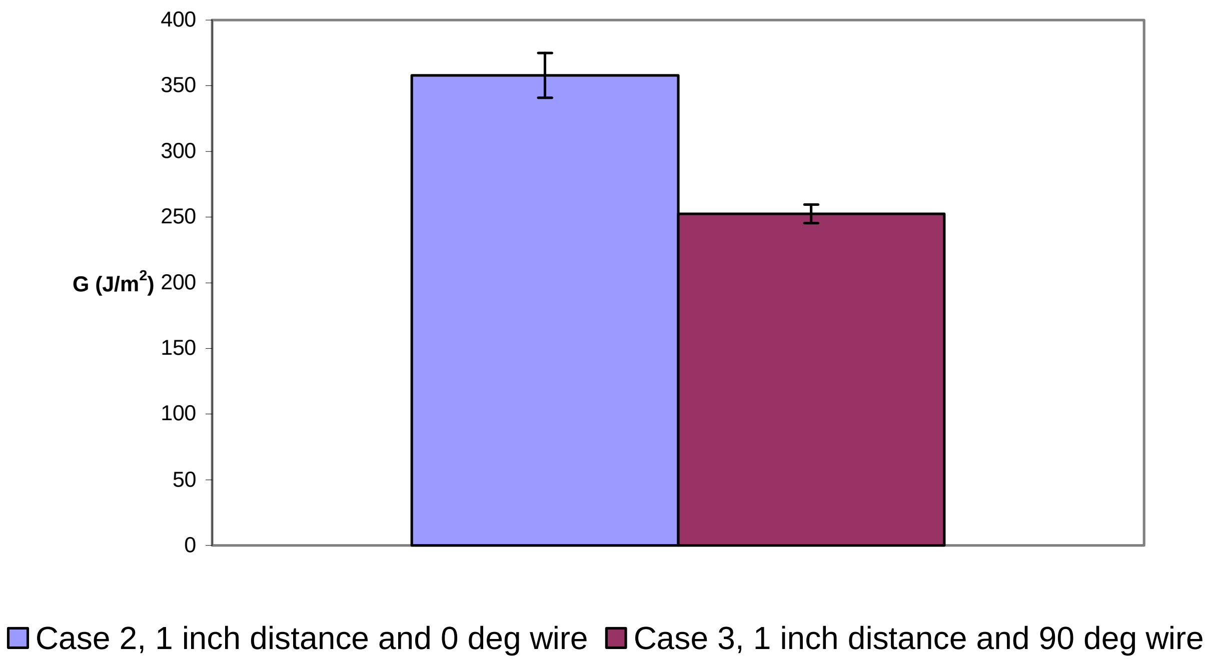

Figure 34. Comparison between Cases 2 and 3

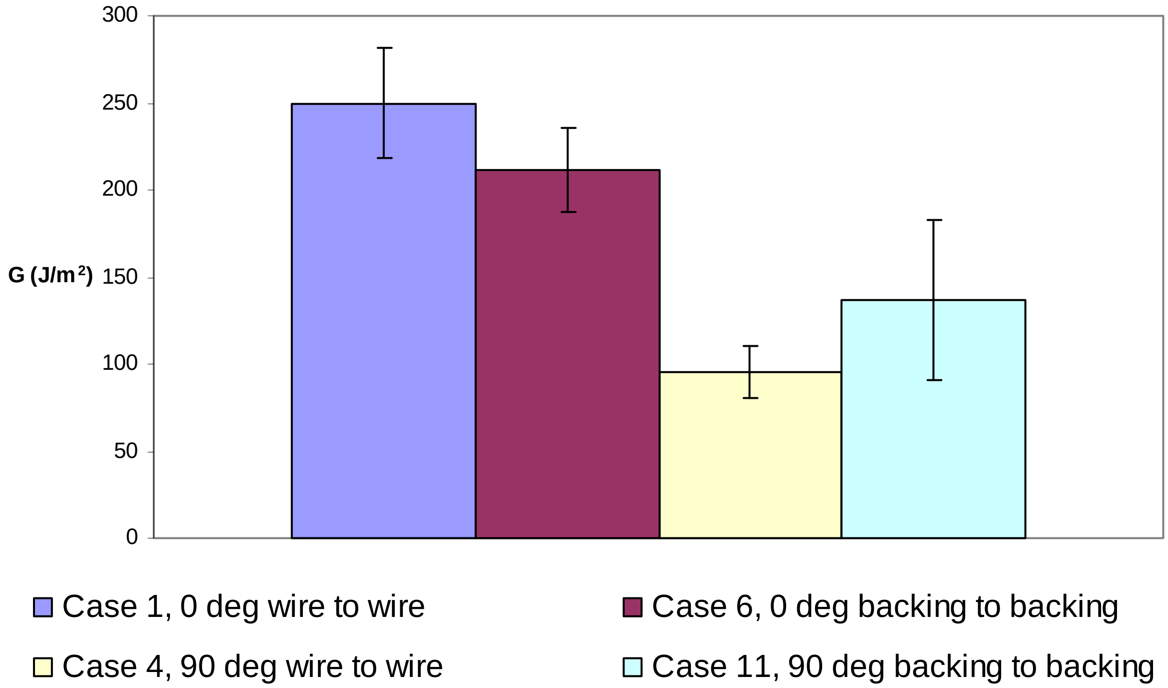

Figure 35. Comparison between Cases 1, 4, 6 and 11

THIS PAGE INTENTIONALLY LEFT BLANK

VI. CONCLUSIONS AND RECOMMENDATIONS

The present experimental study investigated the Mode II fracture toughness of various interfaces of co-cured hybrid composite-metal joints as listed in Figures 26 and 27. The cases in the figures considered a composite-to-composite interface crack, a metal-to-metal interface crack as well as a composite-to-metal interface crack. In addition, the orientations of metal layers were varied between 0 and 90 degrees, and the plastic-backing side of the metal wire layer was also changed to determine its effect on fracture toughness.

Most of interface cracks tested in this study showed more or less similar fracture toughness values as the composite-to-composite interface crack which was used as the baseline. The weakest interface crack was at the location between two 90 degree metal wire layers as shown in Cases 4 and 11. On the other hand, a crack between two 0 degree metal wire layers or between 0 and 90 degree layers did not show much difference in terms of the fracture toughness. A composite-to-composite interface crack, which lies in front of a 90 degree metal wire layer as shown in Cases 2 and 7, had the greater fracture toughness than the pure composite-to-composite interface crack. Among the two, as the crack became closer to the metal layer, the fracture toughness increased.

Based on the study, hybrid composite/metal interface strength was adequate for joining a composite structure to a metallic structure as long as some interface orientations would be avoided, which are potential cracks between two 90 degree metal layers.

Mode I fracture toughness testing as well as mixed mode testing is recommended for future work. Mode I and II and mixed mode fracture propagation along the composite and metal wire interfaces evaluated in this study are the likely failure modes for structural joints constructed of these materials. A complete characterization of the fracture toughness for each of those modes at each of the various interfaces will be necessary to provide comprehensive design information for the development of those joint designs. .

THIS PAGE INTENTIONALLY LEFT BLANK

LIST OF REFERENCES

[1] Stephen M. Graham. "Analysis of a co cured innovative hybrid joint for Marine Composites," presented at SAMPE 2004, May 16-20, Long Beach Convention Center, Long beach, CA Materials and Processing Technology, 60 years of SAMPE progress. Long Beach, California, 2004.

[2] Ashland Composite Polymers, "Composite Polymer Fabrication Tips", Ashland Chemical Corporation, Dublin Ohio, Bulletin #2898, 2005.

[3] Mitsugu Todo, Takashige Nakamura and Kiyoshi Takahashi, "Effects of Moisture Absorption in the Dynamic Interlaminar Fracture Toughness of Carbon/Epoxy Composites," Journal of Composite Materials [Journal]. Vol 34, pp. 630-648, April 1988.

THIS PAGE INTENTIONALLY LEFT BLANK

INITIAL DISTRIBUTION LIST

1. Defense Technical Information Center
   Ft. Belvoir, Virginia

2. Dudley Knox Library
   Naval Postgraduate School
   Monterey, California

3. Professor Young Kwon
   Naval Postgraduate School
   Monterey, California

4. Douglas C. Loup
   Naval Surface Warfare Center, Carderock Division
   West Bethesda, Maryland

5. Erik A. Rasmussen
   Naval Surface Warfare Center Carderock Division
   West Bethesda, Maryland

6. Scott W. Bartlett
   Naval Surface Warfare Center Carderock Division
   West Bethesda, Maryland

7. Engineering and Technology Circular Office, Code 34
   Naval Postgraduate School
   Monterey, California

8. John McWaid
   Integrated Composites Inc.
   Marina California